Published in final edited form as:
J Invest Dermatol. 2009 March ; 129(3): 690–698. doi:10.1038/jid.2008.281.

The EGFR Is Required for Proper Innervation to the Skin

Adel Maklad[1,3], **Jodi R. Nicolai**[1], **Kyle J. Bichsel**[1], **Jackie E. Evenson**[1], **Tang-Cheng Lee**[2], **David W. Threadgill**[2], and **Laura A. Hansen**[1]

1 *Department of Biomedical Sciences, Creighton University School of Medicine, Omaha, Nebraska, USA*

2 *Department of Genetics, University of North Carolina, Chapel Hill, North Carolina, USA*

Abstract

EGFR family members are essential for proper peripheral nervous system development. A role for EGFR itself in peripheral nervous system development *in vivo*, however, has not been reported. We investigated whether EGFR is required for cutaneous innervation using *Egfr* null and skin-targeted *Egfr* mutant mice. Neuronal markers; including PGP9.5, GAP-43, acetylated tubulin, and neurofilaments; revealed that *Egfr* null dorsal skin was hyperinnervated with a disorganized pattern of innervation. In addition, receptor subtypes such as lanceolate endings were disorganized and immature. To determine whether the hyperinnervation phenotype resulted from a target-derived effect of loss of EGFR, mice lacking EGFR expression in the cutaneous epithelium were examined. These mice retained other aspects of the cutaneous *Egfr* null phenotype but exhibited normal innervation. The sensory deficits in *Egfr* null dorsal skin were not associated with any abnormality in the morphology or density of dorsal root ganglion (DRG) neurons or Schwann cells. However, explant and dissociated cell cultures of DRG revealed more extensive branching in *Egfr* null cultures. These data demonstrate that EGFR is required for proper cutaneous innervation during development and suggest that it limits axonal outgrowth and branching in a DRG-autonomous manner.

INTRODUCTION

A richly innervated organ, the skin conveys a multitude of sensory information from different types of cutaneous receptors that function in pain perception, touch, temperature sensing, and vibration sensing. These nerve fibers are organized into a precise pattern of three horizontal nerve plexuses; the subepidermal plexus, deep cutaneous plexus, and the subcutaneous plexus whose perikaria are located in the dorsal root and cranial ganglia (Botchkarev *et al*., 1997, 1999; Maklad *et al*., 2004).

The molecular mechanisms underlying fate acquisition and neurotrophic dependence of neurons conveying different sensory modalities during development have been identified. Neurogenins control the fate of two successive waves of neuroblasts (Ma *et al*., 1998, 1999). Target cells secrete neurotrophic factors that promote the growth and survival of sensory neurons. Developing axons also respond to diverse and largely unidentified environmental cues in reaching specific targets and forming proper patterning of innervation. Many questions about how the peripheral anatomical pattern emerges during development and how the axons reach their synaptic targets remain.

Correspondence: Dr Laura A. Hansen, Department of Biomedical Sciences, Creighton University School of Medicine, 2500 California Plaza, Omaha, Nebraska 68178 USA., E-mail: LHansen@creighton.edu.
[3]Current Address: Department of Anatomy, University of Mississippi Medical Center, Jackson, Mississippi USA.

CONFLICT OF INTEREST
The authors state no conflict of interest.

The EGFR family of receptor tyrosine kinases has been strongly implicated in nervous system development (Birecree *et al*., 1991; Junier, 2000; Casalini *et al*., 2004; for review). All of the family members; including EGFR itself, Erbb2/HER2, Erbb3/HER3, and Erbb4/HER4; are expressed in the nervous system (Casalini *et al*., 2004). *Erbb2*, *Erbb3*, and *Erbb4* null mice reveal roles for these receptors in multiple aspects of neural development. *Erbb2* null mice display a severe loss of sensory and motor neurons and defective formation of the neuromuscular junction, and so lack all cutaneous innervation (Lee *et al*., 1995; Lin *et al*., 2000; Casalini *et al*., 2004). *Erbb2/3* dimers are necessary for Schwann cell development and myelination. *Erbb4* is necessary for pathfinding of the sensory neurons of the cranial ganglia (Golding *et al*., 2000). Taken together, these results implicate the EGFR family in many aspects of nervous system development.

In contrast to the well-defined functions of other family members in peripheral nervous system (PNS) development, little is known about the role of EGFR. The receptor is widely expressed in central and PNS cells, including perineural cells, Schwann cells, and sensory neurons (Werner *et al*., 1988). *Egfr* null mice exhibit defects in neuronal survival and migration in the central nervous system (Threadgill *et al*., 1995). *In vitro* experiments also support a role for EGFR in neuronal and/or glial cell proliferation, survival, differentiation, and neuroprotective potential (Yamada *et al*., 1997). However, the role of EGFR in the development of the PNS has not been explored *in vivo*.

The influence of EGFR in the innervation of developing skin was investigated using two genetic models. Surprisingly, *Egfr* null skin had excessive and disorganized innervation resulting from a primary effect of EGFR in the neuronal compartment. These data demonstrate a surprising and unusual role for a growth factor receptor in the suppression and organization of cutaneous innervation during development.

RESULTS

Egfr null dorsal skin exhibits disorganized hyperinnervation beginning at P0

To determine the role of EGFR in the innervation of the skin, we examined innervation in *Egfr* null and littermate controls between embryonic day 17.5 (E17.5) and postnatal day 18 (P18). No differences in the innervation of the *Egfr* null and control skin were detected at E17.5 (Figure 1). The basic organization of innervation was already established at this time point, including the deep cutaneous plexus (Figure 1a–d, double-headed arrows), the subepidermal plexus (Figure 1c and d, small arrows), and branches from the subepidermal plexus (Figure 1c and d, arrowheads). Immunolabeling using Growth associated protein-43 (GAP-43) antibodies revealed a comparable pattern and density of innervation in the skin of both genotypes at E17.5 (Figure 1). Quantification of PGP9.5 immunolabeled nerve fibers in the dorsal skin was also not significantly different between genotypes at this age (Figure 1e). Thus, no difference in the innervation pattern or density was detected in *Egfr* null dorsal skin at E17.5.

Immunolabeling using GAP-43, PGP9.5, and acetylated tubulin antibodies revealed disorganized patterning and hyperinnervation by postnatal day 0 (P0) in *Egfr* null skin (Figure 2). At this age, the basic innervation pattern of three plexuses in the skin was well established. The deep cutaneous plexus (Figure 2a, c, and e, double-headed arrows) from which radially directed secondary branches emerged (Figure 2a and e, large arrows) and bifurcated to form the subepidermal plexus (Figure 2a, c and e; small arrows) was apparent. From the subepidermal plexus, extensive fine tertiary branches emerged and penetrated the epidermis (Figure 2a, c, and e, arrowheads). In skin lacking EGFR expression, the well-formed deep cutaneous plexus, subepidermal plexus, and the radial fibers connecting them in normal skin were replaced with several horizontal plexuses connected by a random and interlacing network of fibers giving the appearance of rete of nerves with no definite pattern (Figure 2b, d, and f).

The terminal branches to the epidermis were more numerous in the *Egfr* null skin than they were in wild-type littermates (Figure 2f, arrowheads). Fiber quantification revealed significantly higher density of nerve fibers in the P0 *Egfr* null skin with more than twice as many fibers compared to wild-type littermates (Figure 1e).

By P2, the denser and disorganized innervation of the *Egfr* null dorsal skin persisted and became more obvious (Figure S1). Control skin revealed radial bundles that were obliquely oriented and parallel to the hair follicles (Figure S1A, C, and E, large arrows). These radial fibers bifurcated at the dermal–epidermal junction to form the subepidermal plexus (Figure S1A and C, small arrows), from which free nerve endings emerged and penetrated the deeper layers of the epidermis (Figure S1A and E, arrowheads). In the mutant skin, the deep dermal plexus was thicker (Figure S1B and D, double-headed arrows) and located at a deeper level than it is normally (Figure S1A and C, double-headed arrows). The radial fibers were thicker and branched freely before reaching the dermal–epidermal junction. These fibers interlaced and connected to form arcades of nerve fibers that ended directly in the epidermis without forming a subepidermal plexus. The free nerve endings in the basal layer of the epidermis were more profuse compared to those in the wild-type skin (Figure S1B and F, arrowheads).

By P5, the appearance of a more adult pattern in the wild-type dorsal skin (Figure 3a, c, and e) made the denser and disorganized sensory nerves of the mutant skin more obvious (Figure 3b, d, and f). In control skin, the radial fibers that run obliquely and parallel to the hair follicle are now located at regularly spaced intervals (Figure 3a, c, and e, large arrows). Most hair follicles received an afferent bundle from the deep dermal plexus to innervate the lanceolate endings (Figure 3c and e, circles). No branches emerged from the radial bundles except those terminal branches forming the subepidermal plexus (Figure 3a, c, and e, small arrows). The deep dermal plexus was formed of compact bundles of fibers (Figure 3a, double-headed arrows). In *Egfr* null dorsal skin, the normal pattern of innervation was completely absent (Figure 3b, d, and f). The deep cutaneous plexus was thicker, and formed of several defasciculated bundles of fibers (Figure 3b and d, double-headed arrows). The obliquely parallel radial bundles, located at regularly spaced intervals in the controls, were replaced with an extensive network of terminals spanning the entire region between the deep cutaneous and subepidermal plexuses. The free nerve fibers in the epidermis were much more numerous in the mutant epidermis (Figure 3d and f, arrowheads). Fiber density was significantly higher, with a more than twofold increase in the *Egfr* null skin compared to littermate controls (Figure 1e).

Between P5 and P7, only minor changes occurred in the pattern of innervation in the wild-type skin. The deep cutaneous plexus, the radial fibers, subepidermal plexus (Figure S2A, double-headed arrows, large arrows, small arrows, respectively), and the epidermal free nerves (Figure S2C, arrowheads) remained as they were in P5. The density of innervation of the P7 mutant skin, as measured using Image J software, was less than that of P5 mutant skin although still significantly greater than that of the controls (Figure 1e). Manual counting of epidermal free nerve endings confirmed this result and revealed a 60% increase in P7 *Egfr* null skin ($P = 0.0003$, $N = 3$ mice). The disorganized pattern of innervation remained in *Egfr* null skin at P7 (Figure S2B and D). At this age most wild-type hair follicles had mature lanceolate endings as revealed by neurofilament 145 (Nf145) immunolabeling. The mature lanceolate endings surrounded the isthmus region of the follicle as a cuff of interconnected circular fibers (Figure 4a, arrows) and a palisade of short vertical spikes (Figure 4a, small arrows). The palisades emerged from the bottom circular fibers and extended superficially to the top circular band. In the *Egfr* null skin (Figure 4b), the isthmus region contained an extensive bundle of nerve fibers much like the control. However, these fibers branched in different directions, and interlaced without forming circular plexuses or elaborating any vertical spikes in *Egfr* null skin (Figure 4b, arrows). The defects in lanceolate endings persisted to P18. At this age all hairs have

evolved massive lanceolate endings (Figure 4c, arrows). The *Egfr* null lanceolate endings at this age have a poorly developed circular plexus, and rudimentary palisade of few and short vertical spikes (Figure 4d, arrows) in contrast to the wellformed endings in P18 control skin (Figure 4c).

Overall, the innervation pattern of the wild-type skin at 18 days was similar to that of P7 skin. The deep cutaneous plexus (Figure S3A, double-headed arrows), radial fibers now formed of several collateral branches (Figure S3A, large arrows), and subepidermal plexus (Figure S3A and C, small arrows) from which epidermal free nerve endings emerged (Figure S3A and C, arrowheads) were all present. In the null mice, disorganized patterning with increased density of innervation in the region of the superficial half of the dermis persisted (Figure S3B and D), similar to that of P7 null skin. There were denser free nerve terminals in the epidermis of the *Egfr* null skin (Figure S3D, arrowheads). Thus, EGFR expression is necessary for patterning innervation in the skin. In addition and somewhat surprisingly given the functions of other EGFR family members, EGFR reduces the density of innervation in the skin.

Aberrant innervation is restricted to cutaneous targets innervated by dorsal root ganglia

To characterize whether the phenotype obtained by analysis of the hairy dorsal skin is a restricted or generalized effect, we examined the innervation in glabrous foot-pad and whisker-pad skin. PGP9.5 immunolabeling of the foot-pad skin revealed increased free epidermal nerve fibers along with loss of pattern in *Egfr* null mice at P0 and P5 (Figure S4B and D), compared to their wild-type littermates (Figure S4A and C). In contrast to foot-pad skin, indocarbocyanine dye nerve tracing to the whisker pads, revealed no difference in the innervation pattern nor to specific receptor subsets, such as ruffini or corpuscular endings, lanceolate endings, or Merkel's cell endings between genotypes (Figure S4E and F). Similarly, the *Egfr* null intervibrissal skin has a normal innervation pattern (not shown). These data indicate that cutaneous targets supplied by dorsal root ganglion (DRG) were affected whereas cutaneous targets supplied by trigeminal ganglia have normal innervation.

EGFR loss affects only the sensory component of the peripheral nervous system

To understand whether EGFR is required for the entire PNS or to a specific functional component, we analyzed the effect of *Egfr* ablation on sympathetic fibers to autonomic targets in the skin. Tyrosine hydroxylase immunofluorescence of sympathetic fibers in the skin revealed no difference between genotypes in the density or patterning of fibers in dorsal skin at P7, P10, and P14 (Figure S5). These data indicate that EGFR is required only for the sensory component of the PNS contributed by dorsal root ganglia.

Skin-targeted *Egfr* mutant skin has normal innervation

Our data led us to question whether target cell or nervous system EGFR expression was necessary for normal PNS innervation. *Egfr* null skin exhibits severely disorganized hair follicles (Figure 5b), a phenotype that could indirectly impact the patterning of cutaneous innervation. To investigate this possibility, a mouse model was developed that lacked EGFR expression in the epithelium of the skin. As shown in Figure 5a, EGFR expression was reduced in the epithelium of the skin-targeted *Egfr* mutant mice. In contrast to littermate controls (Figure 5d), the skin-targeted mutant mice exhibited disorganized hair follicles within the first week after birth (Figure 5c), similar to those of the *Egfr* null mice (Figure 5b). Consistent with previous publications (Birecree *et al*., 1991; Casalini *et al*., 2004; Koprivica *et al*., 2005), EGFR is expressed in the DRG of control mice (Figure S6). As expected, EGFR expression in the DRG of the skin-targeted mutant and control mice was similar (Figure S6, right), whereas its expression was lacking in *Egfr* null mice (Figure S6, left).

Examination of P14 skin from the skin-targeted *Egfr* mutant mice together with the appropriate littermate controls revealed comparable patterning and density of innervation. In the skin-targeted *Egfr* mutant mice, the deep dermal plexus and subepidermal plexuses, along with the radial fibers and epidermal free nerve plexuses exhibited a normal location and density (Figure 5f and h) in a pattern comparable to the wild-type skin (Figure 5e and g). Neurofilament immunostaining showed a normal location and structure of lanceolate endings; both the horizontal plexuses and vertical palisade in the mutant (Figure 5j) were similar to those of wild-type dorsal skin (Figure 5i). Thus, neither epithelial EGFR expression nor the disorganization of the hair follicles causes the aberrant patterning of innervation in the skin.

Hyperinnervation of *Egfr* null skin results from increased neurite branching in the periphery

The absence of innervation defects in the skin-targeted *Egfr* mutant suggests that the primary defect is in the neural compartment, the DRG. To examine whether the hyperinnervation in *Egfr* null skin is due to increased neuronal perikaria in the DRG, we examined the DRG of *Egfr* null and control mice. EGFR expression was lacking in DRG from *Egfr* null mice (Figure S6, left). DRG populations, namely nerve cells and Schwann cells, were examined in *Egfr* null and control mice using neurofilament 200 and S-100 markers. Neurofilament 200 immunolabeling of the DRG neurons revealed no difference in the cell morphology or density of cell packing between the wild-type and *Egfr* null DRG (Figure 6a and b). Similarly, S-100 immunostaining for Schwann cells revealed no difference between the genotypes (Figure 6c and d). Toluidine blue-stained neuronal cells in the L4/5 DRGs of P5 mutants and their wild-type controls (Figure 6e and f) were counted and no significant difference between the two genotypes was found (numbers indicated below Figure 6e and f). Similarly, electron microscopy revealed no differences in the myelination of *Egfr* null and control axons in the sciatic nerve (not shown). Therefore, the hyperinnervation phenotype in the dorsal skin of *Egfr* null is likely due to increased neurite branching in the periphery.

Egfr null DRG neurons display extensive branching in culture

To test whether ablation of *Egfr* increases neurite branching and outgrowth, DRG from *Egfr* null and littermate control mice were cultured as both whole explants and dissociated cells in culture. Both whole explants and dissociated cells from *Egfr* null mice displayed a more extensive branching pattern in cell culture (Figure 7a–d). Manual counting of the branch points of axonal arbors revealed a significant difference between genotypes. Branch points were increased by 60% ($P = 0.0003$) in *Egfr* null DRG neurons (Figure 7d) compared to controls (Figure 7c). Taken together, the results presented here are consistent with a cell-autonomous role for EGFR in limiting neurite branching during PNS development.

DISCUSSION

In this study, the role of EGFR in the innervation of the skin was investigated. Our data reveal that EGFR is necessary for normal fiber branching and organization during the development of the skin. In the absence of EGFR expression increased branching, hyperinnervation, disorganization of the sensory innervation, and aberrant formation of lanceolate endings to the hair follicles occurred. The normal plexiform arrangement of cutaneous innervation disappeared and was replaced by an extensive network of nerve fibers spanning the entire region between the deep dermal and subepidermal plexuses in systemic *Egfr* null mice. These data suggest that EGFR normally functions as a regulator of pattern formation and an inhibitor of nerve branching during development of cutaneous innervation. The effects of *Egfr* were functionally restricted to the sensory subdivision of the PNS and topographically restricted to DRG neurons. Innervation to sensory targets supplied by cranial ganglia such as trigeminal ganglion and autonomic effectors developed normally in the absence of EGFR.

Several experimental approaches were used to determine whether EGFR regulates cutaneous innervation in a cellautonomous or target-derived manner. Loss of epithelial EGFR expression results in defective epidermal proliferation, disorganization and premature differentiation in the hair follicles, and abnormal hair follicle cycling (Hansen *et al*., 1997; Figure 5). Given the settled notion that a nerve target is an important source of chemotropic (guidance cues), and chemotrophic (neurotrophic support) effects (Goodman and Shatz, 1993; Goodman, 1996; Cook *et al*., 1998), and the defective hair follicles in *Egfr* null skin, the aberrant innervation could have been a secondary effect resulting from target-derived defects. To test this hypothesis, innervation was examined in skin-targeted *Egfr* mutant mice that retain the aberrant hair follicle phenotype due to ablation of cutaneous epithelial EGFR expression. Innervation in skin-targeted *Egfr* mutant mice developed normally, indicating that epithelial expression of *Egfr* is not required for development of cutaneous nerves. However, it is possible that *Egfr* expression in other components in the skin, dermal fibroblasts for example, or other non-neuronal developmental defects in *Egfr* null mice may regulate sensory innervation. Our *in vitro* analysis in which DRG explants and dissociated neurons from *Egfr* null mice displayed extensive terminal arbors argues against such scenarios. The DRGs of the *Egfr* null mice were present in their correct location and in the proper orientation and size comparable to their wild-type littermates. Immunocytochemical labeling for nerve cells and Schwann cell revealed no difference in their morphology or density of cell packing or nerve cell counts in the DRG of the mutant mice. Thus, neuronal expression of *Egfr* appears to regulate nerve branching and pattern formation in a cell-autonomous manner during development of cutaneous innervation. However, conclusive evidence of such autonomous effect should be confirmed by analysis of innervation in DRG-targeted *Egfr* mutant mice.

EGFR loss in the neurons of the DRG may change their behavior or alter the interpretive machinery of their axons to respond to the cues in the skin that would normally inhibit axon growth and branching (Van Horck *et al*., 2002). Consistent with this hypothesis, inhibition of EGFR in the central nervous system blocks the ability of myelin inhibitors and chondroitin sulfate proteoglycans to inhibit neurite outgrowth (Koprivica *et al*., 2005). These authors propose that neuronal EGFR expression is necessary for the ability of myelin to block axon outgrowth. Our data may be consistent with this model for EGFR action. An analysis of the chondroitin sulfate proteoglycan versican in *Egfr* null and control skin did not reveal any differences, however (not shown). Other evidence implicates EGFR activation of phospholipase C-γ, which in turns phosphorylates and deactivates glycogen synthase kinase-3β (Schlessinger, 2000), as a potential mechanism for the phenotype we have observed. A phosphorylated inactive pool of glycogen synthase kinase-3β localizes to the tip of the growth cone and confers competence to respond to the repulsive axon guidance molecule semaphorin 3A (Eickholt *et al*., 2002). EGFR activation of glycogen synthase kinase-3β may regulate the interpretive machinery of DRG neurons to inhibitory axon guidance and branching cues in the skin. Consequently, EGFR loss in the DRG neurons may result in defective responsiveness to the inhibitory cues, leading to massive branching and loss of normal pattern formation in *Egfr* null skin.

The absence of abnormalities in the DRG in the presence of aberrant innervation of the dorsal skin of the null mice suggests that EGFR is not involved in the early events of neurogenesis of the PNS such as cell migration, proliferation, or cell death. It rather suggests that EGFR controls specific aspects of cell behavior during development such as neurite extension and branching in a cell-autonomous fashion. This is in striking contrast to the effects of other EGFR family members. In *Erbb2* and *Erbb4* mutants, there is massive loss of the neurons in DRG and cranial ganglia due to cell death and abnormal migration of the neural crest in a nonautonomous fashion by the Schwann cell population (Lee *et al*., 1995; Lin *et al*., 2000; Golding *et al*., 2000). *Erbb3* null mice lack the enteric nervous system due to abnormal migration of the neural crest cells (Riethmacher *et al*., 1997; Britsch *et al*., 1998). EGFR

appears to function much later in development when compared to other family members. Thus, our data and those of others reveal quite distinct roles for EGFR family members and suggest that the various family members may function in concert or sequentially, autonomously, and nonautonomously, to regulate distinct aspects of cell behavior during development of the PNS.

MATERIALS AND METHODS

Animals

Egfr null mice were obtained by breeding mice heterozygous for the receptor and genotyped using PCR as previously published (Threadgill *et al*., 1995). To obtain mice lacking EGFR expression in the epithelium of the skin, keratin 14 promoter-driven *Cre recombinase* transgenic mice (Jackson Labs, Bar Harbor, MA) were crossed with mice containing loxP sites flanking exon 2 of the *Egfr* gene. The loxP *Egfr* construct was designed to generate a frameshift when splicing between exon 1 and downstream exons occurs. The mice were backcrossed to generate *Cre recombinase*$^{+/-}$/*Egfr*$^{fl/fl}$ mice, referred to here as skin-targeted *Egfr* mutant mice. DNA was extracted from tail snips and mice genotyped using PCR. Primers for the skin-targeted *Egfr* mutant mice included 5′-ACACTAGCACTGACTGCTGG-3′ and 5′-GGCGAGATAAACCCAAAGCA-3′ (*Egfr* loxP allele) and 5′-ACCAGCCAGCTATCAACTCG-3′, 5′-TTACATTGGTCCAGCCACC-3′, 5′-CTAGGCCACAGAATTGAAAGATCT-3′, and 5′-GTAGGTGGAAATTCTAGCATCATCC-3′ (keratin 14-driven *Cre recombinase*). To obtain E17.5 embryos, male and female mice were housed together for 12 hours, and then female mice were checked for vaginal plugs. Female mice with plugs were designated pregnant at embryonic day 0.5. Pregnant female mice were killed at 17.5 days and embryos were removed. All animal procedures were approved by the appropriate institutional animal care and use committee and performed in compliance with American Association of Laboratory Animal Care guidelines.

Analysis of Skin Innervation

Cutaneous innervation was examined in skin from mice transcardially perfused with 4% paraformaldehyde in phosphate-buffered saline after killing. Samples were postfixed in 4% paraformaldehyde in phosphate-buffered saline until the time of use. Skin was cryoprotected in 30% sucrose in phosphate-buffered saline for 4 hours and embedded in OCT.

Immunofluorescence was performed on floating 40 μm thick cryostat sections using standard techniques including antigen retrieval (Vector Laboratory, Burlingame, CA) and incubation with the primary antibody for 72 h at 4 °C. The primary antibodies used included anti-acetylated tubulin (1:250; Sigma, St Louis, MO), anti-neurofilament 145 (1:200; Chemicon International, Temecula, CA), PGP9.5 (1:2,000; Chemicon International), anti-GAP-43 (1:2,000; Chemicon International), and tyrosine hydroxylase (1:500; Chemicon International). Skin sections were incubated with Alexa Fluor 488-conjugated goat anti-rabbit secondary antibodies (1:1,000; Invitrogen, Carlsbad, CA) and were mounted. Z series of images were collected using a confocal microscope (Zeiss LSM 510 META NLO system, Thornwood, NY) and collapsed in one focal plane using confocal software.

Quantification of sensory fibers

PGP9.5-labeled fibers were quantified in photographs taken at × 20 magnification, using NIH ImageJ software (Developed at the National Institutes of Health and available on the Internet at http://rsb.info.nih.gov/nih-image/). Ten skin sections were examined for each of three animals per group. In each section, three randomly selected microscopic fields were photographed with the epidermis parallel to the long edge of the photo. Using Image J software, the total area of the PGP9.5-positive fibers was quantified in each image and the mean for each

mouse was calculated. Fiber counting was restricted to the fibers of the deep dermal and subepidermal plexuses with the investigator blinded as to the identity of the sample. Differences in innervation between the genotypes were statistically analyzed using a Student's *t*-test. Manual counting of the epidermal free nerve endings was also performed in P7 skin ($N = 3$ mice) as described in Hendrix *et al*. (2008). In both digital and manual counting a strictly standardized protocol for tissue-harvesting location, sectioning orientation, immunofluorescence protocols, microscopic field selection, laser intensity, and gain, was followed as described in Hendrix *et al*. (2008).

DRG cell counts and immunostaining

The fourth and fifth lumbar dorsal root ganglia (L4 and L5) of P5 mice were used to count DRG nerve cell number ($N = 3$ mice). L4 and L5 lumbar DRGs were removed and cryoprotected in 30% sucrose in phosphate-buffered saline for 2 hours. Ganglia were embedded in OCT and 10 μm thick serial sections were stained with toluidine blue. Nerve cells are readily distinguishable morphologically from other populations such as Schwann cells and fibroblasts. Every other section was photographed at × 10 magnification and the cells were counted. The mean number and standard deviation of nerve cells in L4 and L5 DRG from each mouse were determined, and differences were also determined using a Student's *t*-test. Some L3 and L5 DRGs were embedded in gelatin, vibratome sectioned at 30 μm thick sections and processed for immunostaining with anti-neurofilament 200 (1:200; Chemicon International) and anti-S-100 (1:500; Dako, Carpinteria, CA).

DRG tissue culture, and neurite branching assay

Ganglia from all spinal levels of P1 pups were dissected as described above. DRGs from five animals for each genotype were pooled together. DRGs were digested in 0.25% trypsin for 45 minutes to dissociate cells. Cells were plated in tissue culture plates at a density of 200,000 cells per 60mm well in DMEM (Invitrogen) with 10% fetal bovine serum. In some experiments, whole DRG were explanted. Cells were re-fed the next day and at 48 hours intervals thereafter. After 4 days, cells were fixed in 4% paraformaldehyde for 30 minutes. Cells were immunolabeled using PGP9.5 antibodies as described above for skin, and counterstained with 46-diamidino-2- phenyl indole (Vector Laboratory). Images were collected using a × 4 objective on the confocal microscope. Branch points were counted as described elsewhere (Luo *et al*., 2002).

Immunoblotting

Epidermis was removed using the heat-shock method as described by Hansen *et al*., (1997). Immunoblotting was performed using standard techniques and EGFR (Santa Cruz Biotechnology, Santa Cruz, CA) and actin (Sigma) antibodies.

Supplementary Material

Refer to Web version on PubMed Central for supplementary material.

Acknowledgements

We thank Dr Bernd Fritzsch for his helpful suggestions and editing of the finished paper. This publication was supported by the National Institutes of Health (P20 RR-02-003). This investigation was conducted in a facility constructed with support from Research Facilities Improvement Program grant number 1 CO6 RR17417-01 from the National Center for Research Resources, National Institutes of Health.

Abbreviations

DRG

dorsal root ganglion

E17.5
embryonic day 17.5

GAP-43
growth-associated protein 43

Nf145
neurofilament 145

P0
postnatal day 0

PNS
peripheral nervous system

References

Birecree E, King LE, Nanney LB. Epidermal growth factor and its receptor in the developing human nervous system. Brain Res Dev Brain Res 1991;60:145–54.

Botchkarev VA, Eichmuller S, Johansson O, Paus R. Hair cycledependent plasticity of skin and hair follicle innervation in normal murine skin. J Comp Neurol 1997;29:379–95. [PubMed: 9303424]

Botchkarev VA, Peter EM, Botchkareva NV, Maurer M, Paus R. Hair cycle-dependent changes in adrenergic skin innervation, and hair growth modulation by adrenergic drugs. J Invest Dermatol 1999;113:878–87. [PubMed: 10594725]

Britsch S, Li L, Kirchhoff S, Theuring F, Brinckmann V, Birchmeier C, et al. The ErbB2 and ErbB3 receptors and their ligand, neuregulin-1, are essential for development of the sympathetic nervous system. Genes Dev 1998;12:825–36.

Casalini P, Iorio MV, Galmozzi E, Menard S. Role of HER receptors family in development and differentiation. J Cell Physiol 2004;200:343–50. [PubMed: 15254961]

Cook G, Tannahill D, Keynes R. Axon guidance to and from choice points. Curr Opin Neurobiol 1998;8:64–72. [PubMed: 9568393]

Eickholt BJ, Walsh FS, Doherty P. An inactive pool of GSK-3 at the leading edge of growth cones is implicated in Semaphorin 3A signaling. J Cell Biol 2002;157:211–7. [PubMed: 11956225]

Golding JP, Trainor P, Krumlauf R, Gassmann M. Defects in pathfinding by cranial neural crest cells in mice lacking the neuregulin receptor ErbB4. Nat Cell Biol 2000;2:103–9. [PubMed: 10655590]

Goodman CS. Mechanisms and molecules that control growth cone guidance. Annu Rev Neurosci 1996;19:341–77. [PubMed: 8833447]

Goodman CS, Shatz CJ. Developmental mechanisms that generate precise patterns of neuronal connectivity. Cell 1993;72:77–98. [PubMed: 8428376]

Hansen LA, Alexander N, Hogan MF, Sundberg JP, Dlugosz A, Threadgill DW, et al. Genetically null mice reveal a central role for epidermal growth factor receptor in the differentiation of the hair follicle and normal hair development. Am J Pathol 1997;150:1959–75. [PubMed: 9176390]

Hendrix S, Picker B, Liesmann C, Peters EM. Skin and hair follicle innervation in experimental models: a guide for the exact and reproducible evaluation of neuronal plasticity. Exp Dermatol 2008;17:214–27. [PubMed: 18261087]

Junier MP. What role(s) for TGFalpha in the central nervous system? Prog Neurobiol 2000;62:443–73. [PubMed: 10869779]

Koprivica V, Cho KS, Park JB, Yiu G, Atwal J, Gore B, et al. EGFR activation mediates inhibition of axon regeneration by myelin and chondroitin sulfate proteoglycans. Science 2005;310:106–10. [PubMed: 16210539]

Lee KF, Simon H, Chen H, Bates B, Hung MC, Hauser C. Requirement for neuregulin receptor erbB2 in neural and cardiac development. Nature 1995;378:394–8. [PubMed: 7477377]

Lin W, Sanchez HB, Deerinck T, Morris JK, Ellisman M, Lee KF. Aberrant development of motor axons and neuromuscular synapses in erbB2-deficient mice. Proc Natl Acad Sci USA 2000;97:1299–304. [PubMed: 10655525]

Luo ZJ, King RH, Lewin J, Thomas PK. Effects of nonenzymatic glycosylation of extracellular matrix components on cell survival and sensory neurite extension in cell culture. J Neurol 2002;249:42431.

Ma Q, Fode C, Guillemont F, Anderson DJ. Neurogenin1 and neurogenin2 control two distinct waves of neurogenesis in developing dorsal root ganglia. Genes Dev 1999;13:1717–28. [PubMed: 10398684]

Ma Q, Chen Z, del Barco Barrantes I, de la Pompa JL, Anderson DJ. Neurogenin1 is essential for the determination of neuronal precursors for proximal cranial sensory ganglia. Neuron 1998;20:469–82. [PubMed: 9539122]

Maklad A, Fritzsch B, Hansen LA. Innervation of the maxillary vibrissae in mice as revealed by anterograde and retrograde tract tracing. Cell Tissue Res 2004;315:167–80. [PubMed: 14610665]

Riethmacher D, Sonnenberg-Riethmacher E, Brinckmann V, Yamaai T, Lewin GR, Birchmeier C. Severe neuropathies in mice with targeted mutations in the ErbB3 receptor. Nature 1997;389:725–30. [PubMed: 9338783]

Schlessinger J. Cell signaling by receptor tyrosine kinases. Cell 2000;103:211–25. [PubMed: 11057895]

Threadgill DW, Dlugosz AA, Hansen LA, Tennenbaum T, Lichti U, Yee D, et al. Targeted disruption of mouse EGF receptor: effect of genetic background on mutant phenotype. Science 1995;269:230–4. [PubMed: 7618084]

Van Horck FP, Lavazais E, Eickholt BJ, Moolenar WH, Divecha N. Essential role of type I(alpha) phosphatidylinositol 4-phosphate 5-kinase in neurite remodeling. Curr Biol 2002;12:241–5. [PubMed: 11839279]

Werner MH, Nanney LB, Stoscheck CM, King LF. Localization of immunoreactive epidermal growth factor receptors in human nervous system. J Histochem Cytochem 1988;36:81–6. [PubMed: 3275713]

Yamada M, Ikeuchi T, Hatanaka H. The neurotrophic action and signalling of epidermal growth factor. Prog Neurobiol 1997;51:19–37. [PubMed: 9044427]

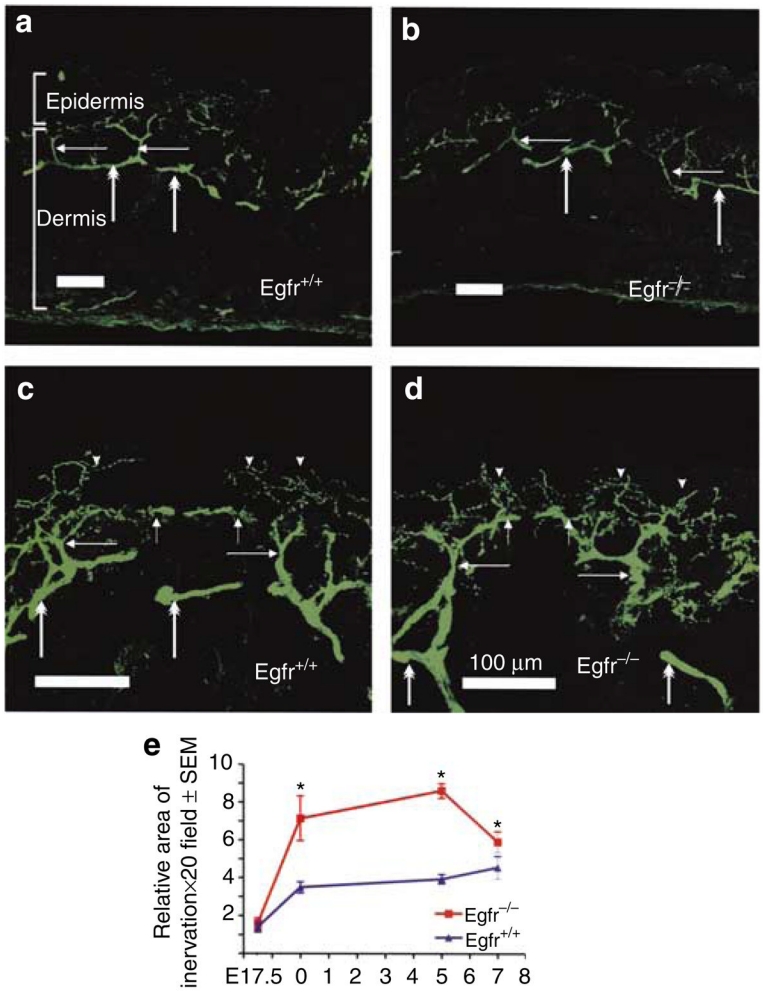

Figure 1. Ablation of *Egfr* disturbs cutaneous innervation after E17.5

(**a**–**d**) GAP-43 immunofluorescence (green) shown in E17.5 skin. (**a**) Photomicrograph of skin section showing normal organization of sensory nerves of the skin in the wild type. Note that the normal pattern of nerve plexuses has emerged at this age; the deep dermal plexus (double-headed arrows), and radial fibers (large arrows). (**b**) Photomicrograph of skin section of the *Egfr* null. Note the lack of difference between innervation pattern and density between the wild-type skin (**a**) and the mutant. (**c**) A higher magnification image of skin section showing the deep dermal plexus (double-headed arrows), the radial bundles (large arrows), subepidermal plexus (small arrows), and epidermal free nerve endings (arrowheads). (**d**) The deep dermal plexus (double-headed arrows), the radial fibers (large arrows), subepidermal plexus (small arrows), and epidermal free nerve endings in *Egfr* null skin in a pattern and density comparable to the wild-type skins in (**c**). Scale bar is 100 μm (**a–d**). (**e**) The density of innervation is increased the skin of *Egfr* null mice beginning at P0. Nerve fiber density was quantified in PGP9.5- immunostained dorsal skin sections as described in the Materials and Methods. The relative area of PGP9.5-positive fibers was determined in 30 microscopic fields for each of three mice in each group. The mean for each mouse was calculated and the average area of innervation for each genotype at several time points is shown. Asterisk (*) indicates the mean is significantly different in the *Egfr* null skin compared to the corresponding wild-type control, where $P \leq 0.05$.

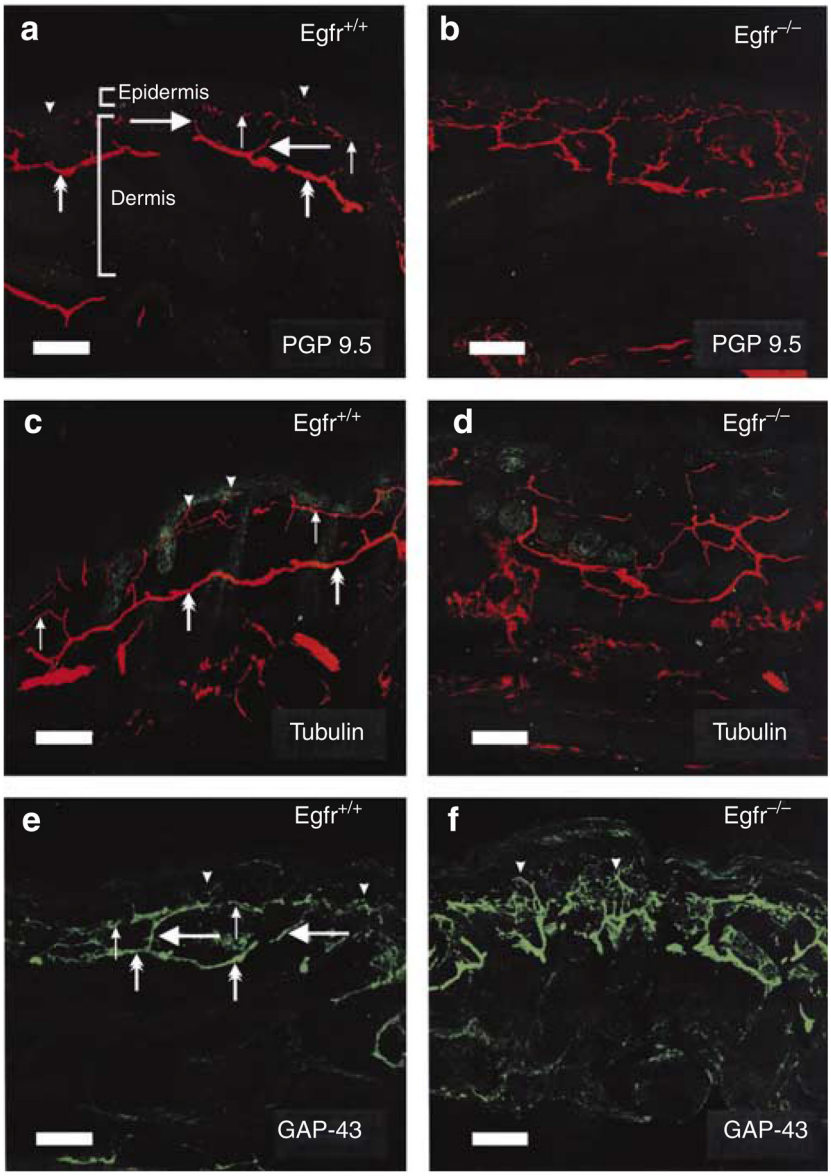

Figure 2. Sensory innervation is disorganized in P0 dorsal skin from *Egfr* null mice

(a) Photomicrographs of cutaneous sensory nerves in control mouse skin, labeled with PGP9.5, showing normal organization of sensory nerves into deep dermal plexus (double-headed arrows), radial fibers (large arrows), subepidermal plexus (small arrows), and epidermal free nerve endings (arrowheads). (**b**) Cutaneous innervation of *Egfr* null skin. Note the increased density and absence of normal pattern. The normal plexiform arrangement was replaced by a rete of nerves throughout the superficial layer of the dermis. (**c**) Acetylated tubulin immunolabeled sensory nerves of the wild-type skin showing the normal pattern of deep dermal plexus (double-headed arrows), subepidermal plexus (small arrows), and epidermal free nerve branches (arrowheads). (**d**) Acetylated tubulin immunolabeling of the cutaneous nerves of *Egfr* null showing consistently denser and disorganized pattern of sensory fibers. Note that epidermal and follicular keratinocytes (green cells) are immunostained for keratin 14 (K14) in (**c**) and (**d**). (**e**) Normal innervation pattern of the wild-type skin as revealed by GAP-43 immunolabeling. (**f**) Cutaneous innervation of *Egfr* null showing denser and disorganized pattern with GAP-43 immunolabeling. Scale bar is 100 μm in all figures.

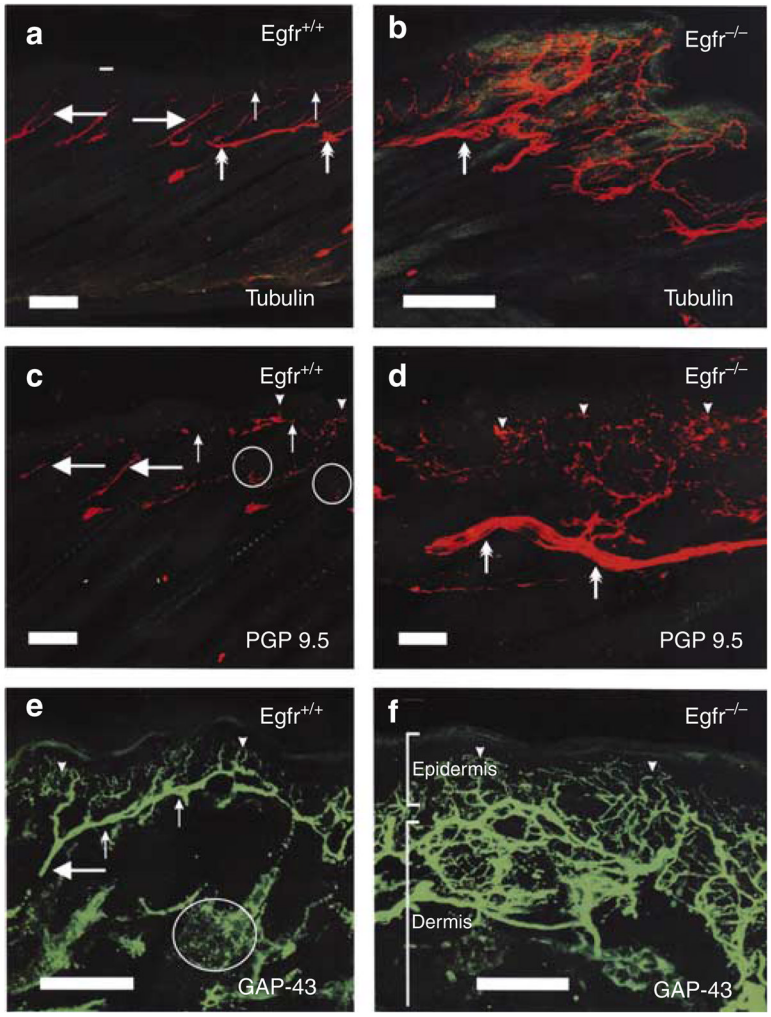

Figure 3. Increased and disorganized sensory innervation in P5 *Egfr* null dorsal skin

(a, c, e) Acetylated tubulin, PGP9.5, and GAP-43 immunolabeled sensory nerves of the wild-type skin. The deep dermal plexus (double-headed arrows), and the subepidermal plexus (small arrows) are parallel to the skin surface. The radial fibers (large arrows) are obliquely oriented and parallel to the hair follicles, and are located at regularly spaced intervals. The lanceolate endings (circles) have started to form around several hair follicles. (**b**, **d**, **f**) Sensory nerves in the *Egfr* null skin. The normal three horizontal plexuses are replaced by single thick horizontal plexus (double-headed arrow) in the mid dermis, from which extensive set of radial fibers freely interlacing with massive secondary terminals. Note the extensive branching of the free nerve ending in the epidermis arrowheads in (**d**). Scale bar is 100 μm in all figures.

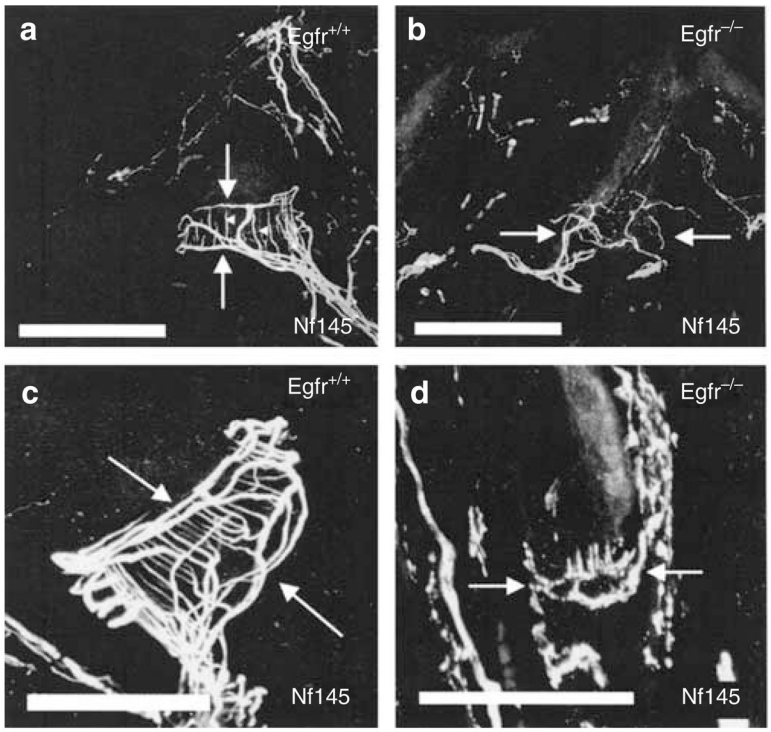

Figure 4. *Egfr* null skin exhibits immature and disorganized lanceolate endings

(**a**) Neurofilament-labeled normal, mature lanceolate ending in wild-type P7 skin, with its circular fibers (arrows) and vertical palisade (arrowheads). (**b**) A malformed lanceolate ending in P7 *Egfr* null skin (arrows). Note the absence of palisade and aberrant circular fibers. (**c**) Neurofilament staining of a mature lanceolate ending (arrows) in P18 control skin. (**d**) Malformed lanceolate ending in P18 *Egfr* null skin (arrows). Scale bar is 100 μm in all figures.

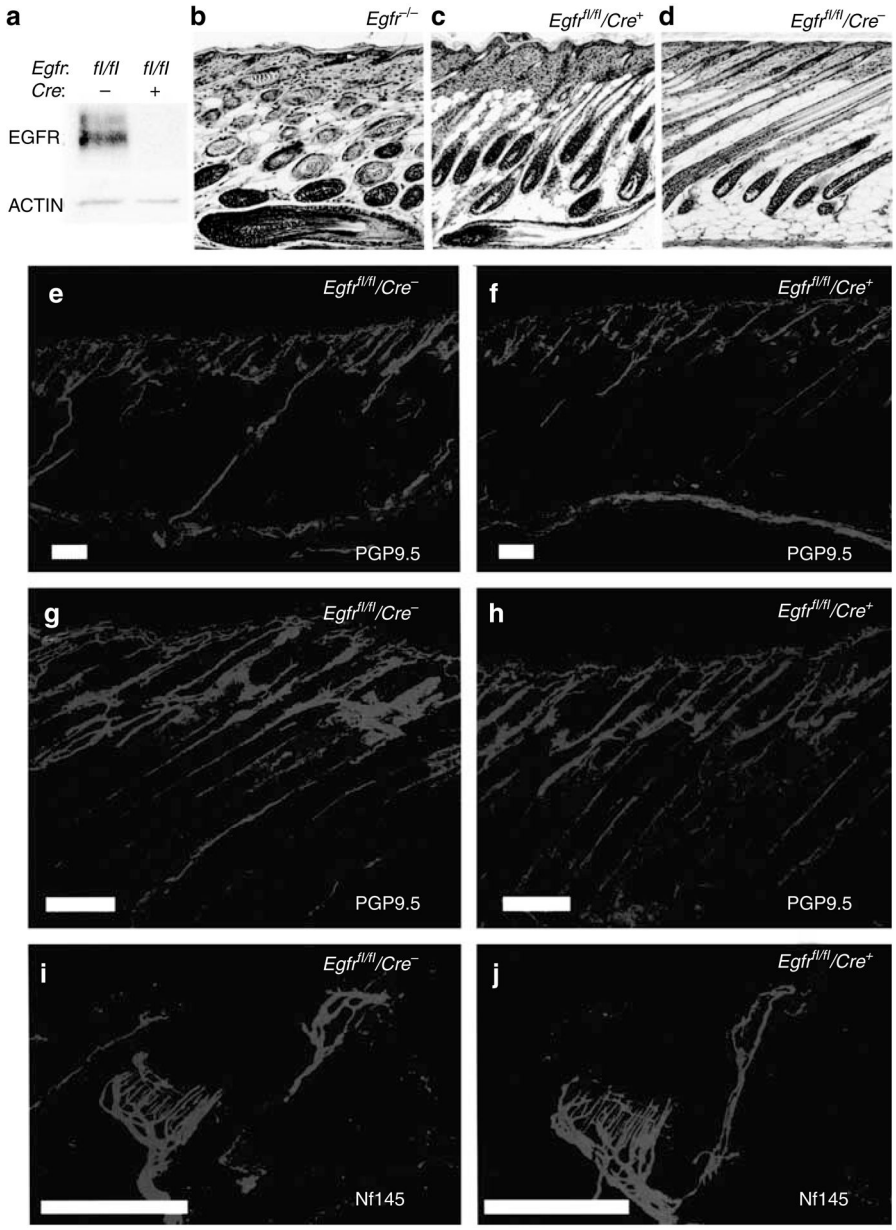

Figure 5. Ablation of *Egfr* in the epithelium of the skin results in disorganized hair follicles but normal innervation

(a) Immunoblotting of skin-targeted *Egfr* mutant ($Egfr^{fl/fl}/Cre^{+}$) epidermis demonstrates loss of EGFR protein when compared to control ($Egfr^{fl/fl}/Cre$). Bar graph indicates relative EGFR signal normalized to actin from densitometry of immunoblots ($N = 14$ mice). Hematoxylin and eosin-stained skin sections from 7- to 8-day-old *Egfr* null (**b**) and skin-targeted *Egfr* mutant mice (**c**) exhibit disorganized hair follicles when compared to the normal control (**d**). PGP9.5-labeled (**e–h**) and neurofilament-labeled (**i**, **j**) nerve fibers of 14 day-old skin-targeted mutant dorsal skin (**f**, **h**, **j**) show normal innervation. Note that the deep dermal plexus, subepidermal plexus, radial fibers, and lanceolate endings are comparable to those in the wild type at 14 day (**e**, **g**, **i**). Scale bar is 100 μm in all figures.

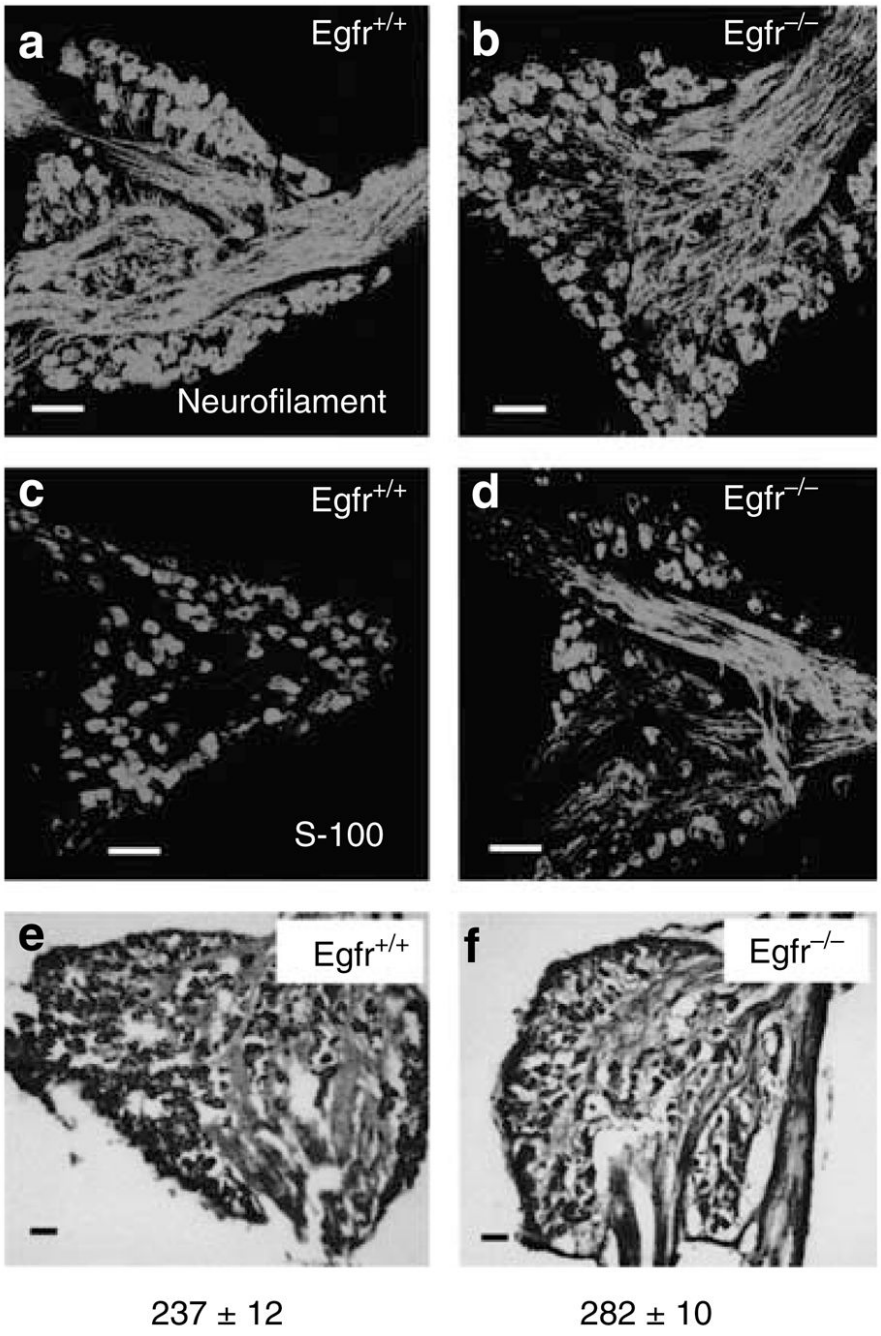

Figure 6. Analysis of *Egfr* null and wild-type DRG reveals no differences

(**a**, **b**) Neurofilament 200-immunostained neurons of the wild-type and *Egfr* null Mid-DRG section at P5. Note the absence of any morphological difference or any difference in the density of neurons. (**c**, **d**) S-100-immunostained Schwann cells of wild-type and null Mid-DRG sections at P5, showing size and density similarity in both genotypes. (**e**, **f**) Toluidine-blue-stained wild-type and null P5 DRG sections for cell counting. Cells were quantified as described in the Materials and Methods and numbers indicate mean DRG cells±SEM. $N = 3$ mice. No significant difference between genotypes was detected using a Student's *t*-test.

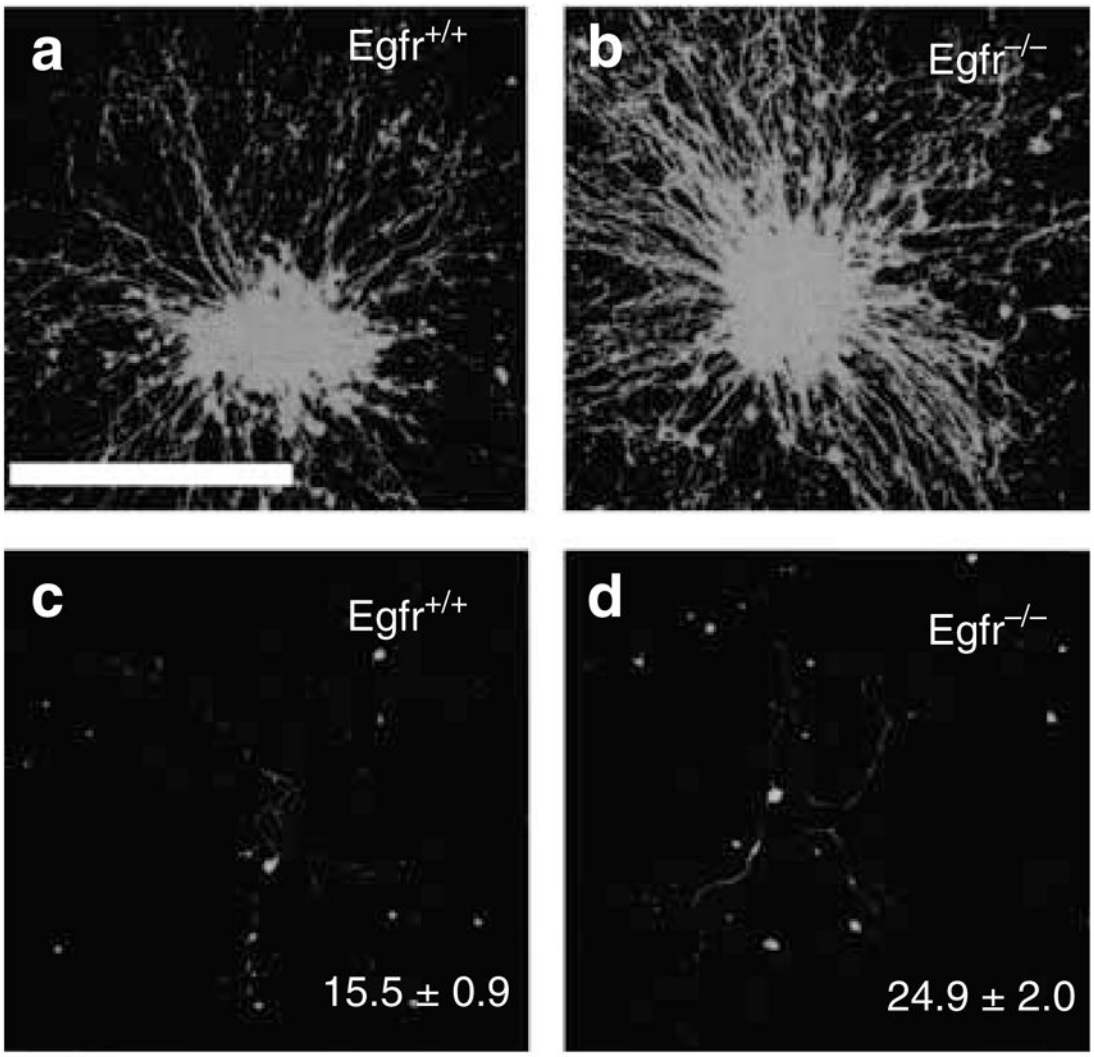

Figure 7. DRG explants and dissociated cells display aberrant branching upon ablation of *Egfr*

(a) Photomicrograph of wild-type P0 whole DRG explant after 4 days in culture, and labeling with PGP9.5. (**b**) *Egfr* null P0 DRG explant displays more branches than the wild-type littermate. Wild-type (**c**) and *Egfr* null (**d**) P0 dissociated DRG neurons labeled with PGP9.5. The *Egfr* null neurons demonstrate significantly increased branching compared to the littermate controls. Numbers indicate mean branch points ±SEM quantified as described in the Materials and Methods. Mean for the *Egfr* null is significantly greater than for the controls using a Student's *t*-test, where $P \leq 0.0001$. $N = 30$ cells. Scale bar is 1 mm.